The Astrophysical Journal, 850:69 (4pp), 2017 November 20 https://doi.org/10.3847/1538-4357/aa9274

Gas-phase Absorptions of $C_{42}H_{18}^+$ near 8300 Å below 10 K: Astronomical Implications

E. K. Campbell and J. P. Maier

Department of Chemistry, University of Basel, CH-4056 Basel, Switzerland; ewen.campbell@unibas.ch, j.p.maier@unibas.ch

Received 2017 July 12; revised 2017 September 12; accepted 2017 October 8; published 2017 November 17

Abstract

The gas-phase electronic spectrum of $C_{42}H_{18}^+$ (HBC^+) with an origin band at 8281 Å has been measured below 10 K by photofragmentation of helium complexes ($C_{42}H_{18}^+$–He_n) in a radiofrequency trap. HBC^+ is a medium-sized polycyclic aromatic hydrocarbon (PAH) cation, and using an ion trapping technique it has been possible to record a high-quality gas-phase spectrum to directly compare with astronomical observations. No diffuse interstellar bands (DIBs) have been reported at the wavelengths of the strongest absorption bands in the $C_{42}H_{18}^+$ spectrum. Measurement of absolute absorption cross sections in the ion trap allows upper limits to the column density of this ion to be 10^{12} cm^{-2}, indicating that even PAH cations of this size, which are believed to be stable in the interstellar medium, should be excluded as candidates for at least the strong DIBs.

Key words: ISM: molecules

1. Introduction

Polycyclic aromatic hydrocarbons (PAHs) are thought to be prevalent in a number of interstellar environments, locking up 10%–20% of the available carbon (Tielens 2008). The main evidence cited for their presence is the emission features in the infrared, often labeled as aromatic infrared bands (AIBs). The broadness of the infrared fluorescence means that no individual molecule is likely to be identified, but the dominant features at 3.3, 6.2, 7.7, 8.6, and 11.2 μm are similar to the infrared frequencies of PAHs. The current opinion is that the AIBs are likely to be due to PAH species comprising 50–100 carbon atoms.

On the other hand, there are around 600 distinct absorption features in the optical region that are observed toward reddened stars, known as diffuse interstellar bands (DIBs). Unlike the AIBs, it is likely that one molecule contributes to just a few of the DIBs, therefore it should be possible to identify them individually by comparison with laboratory spectra recorded under similar conditions to those prevailing in the diffuse clouds, as recently shown for C_{60}^+ (Campbell et al. 2015, 2016b; Walker et al. 2017). Thus, it is of some interest to also obtain the electronic spectra of a few large PAH cations, because in the diffuse medium they are likely to be ionized. Such spectra of sufficient quality for a comparison with DIB data have now been obtained for cations of typical aromatics including corranulene, $C_{20}H_{10}^+$, and coronene, $C_{24}H_{12}^+$, and led to the conclusion that species of this size are not among the carriers responsible for the stronger DIBs (Hardy et al. 2017). It is also a matter of contention whether the AIB emission bands and DIBs are related to similar type of molecules.

$C_{42}H_{18}^+$ is a PAH cation with an all-benzenoid structure. These possess an increased stability compared with other isomers and this has been suggested as a mechanism through which the selection of a few structures, among numerous possible ones, could arise and lead to an increased relative abundance in the interstellar medium (Kokkin et al. 2008). Astrochemical interest in this ion also stems from the fact that such sizes have been modeled to be stable in the interstellar medium, in contrast to smaller species that would undergo dehydrogenation (Le Page et al. 2003). There is a report of the electronic absorption spectrum of an even larger PAH^+, $C_{78}H_{26}^+$ (Zhen et al. 2016), but due to the technique used the data are of insufficient quality to compare directly with astronomical observations.

In this paper, we report on the cold gas-phase laboratory spectrum of $C_{42}H_{18}^+$–He in the near-infrared. This spectrum was obtained using a cryogenic ion trap, relying on the loss of the helium atom for the detection. The small shift induced by the helium was evaluated experimentally and the absorption spectrum of $C_{42}H_{18}^+$ at low interstellar temperatures was thus obtained and compared with astronomical data. Absorption cross-section measurements are also presented, enabling a quantitative discussion of the astrophysical relevance of PAH^+ species of this size.

2. Experimental

Experiments were carried out using the cryogenic 4-pole radiofrequency ion trap apparatus described in Campbell et al. (2016a). Cations of HBC, $C_{42}H_{18}^+$, are generated in an electron impact ionization source after heating a solid sample to 315°C. After passing through a quadrupole mass filter, the ions are turned through 90° and injected into a linear quadrupole ion trap ($V_0 = 160$ V, $f = 780$ kHz) where the temperature of the trap walls is 4 K. The stored ions (10^2–10^3/filling) are cooled *via* collisions with cold helium buffer gas, introduced into the trap by resonant excitation of a piezo valve for 500 ms, leading to number densities of some 10^{15} cm^{-3}. The collisions relax the internal degrees of freedom of $C_{42}H_{18}^+$ to below 10 K. Under these conditions weakly bound helium complexes, $C_{42}H_{18}^+$–He_n, are also formed. After pumping out the buffer gas for several hundred milliseconds the ion cloud is irradiated for 50 ms by a continuous wave (cw) Ti:Sap laser ($\Delta\lambda \approx 0.2$ Å). The trap contents are extracted and analyzed using a quadrupole mass spectrometer and a Daly detector, with the process repeated at a rate of 1 Hz. Photofragmentation spectra of $C_{42}H_{18}^+$–He are recorded by monitoring an attenuation in the number of ions at $m/z = 526$.

The number of complexes stored in the trap is N_0 before irradiation and $N(\Phi)$ following exposure to laser light with fluence Φ. The attenuation is $1 - N(\Phi)/N_0$ and a reference signal is measured on alternate trapping cycles without laser radiation. The data presented in Figure 1 have been normalized

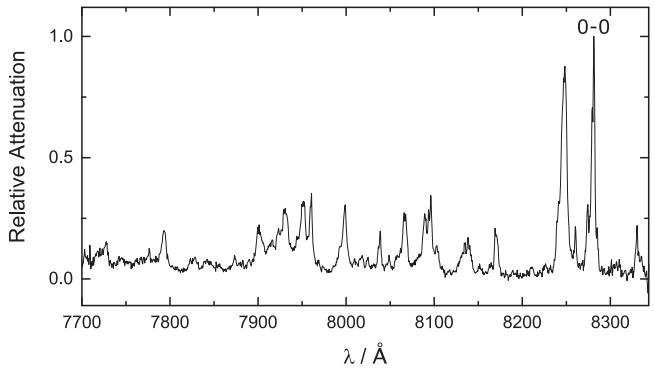

Figure 1. Electronic spectrum of $C_{42}H_{18}^{+}$–He below 10 K. The weak band at 8331 Å is assumed to arise due to a lower energy transition.

such that the relative attenuation of the strongest band is equal to unity. Information on absorption cross sections is obtained by monitoring the number of complexes as a function of the laser fluence to which they are exposed, according to the description given previously (Campbell et al. 2016a, 2017). The data are fitted to the exponential function $N(\Phi) = N_0 \exp(-\Phi/\Phi_0)$ from which the characteristic fluence, Φ_0, is determined. With the latter expressed in units of mJ per cm^2 the cross section is given by $\sigma = h\nu/\Phi_0$, where $h\nu$ is the photon energy.

3. Gas-phase Spectrum of $C_{42}H_{18}^{+}$–He below 10 K

The electronic spectrum of HBC^+ in a 6 K neon matrix was reported by Steglich et al. (2011). The observed gas-phase spectrum of $C_{42}H_{18}^{+}$–He (Figure 1) has two strong bands with maxima at 8281 and 8248 Å. There are numerous other absorptions toward higher energy that correspond to transitions to various vibrational levels in the excited electronic state(s). Calculations indicate that the lowest-energy electronic transition of HBC^+ lies at wavelengths longer than around 2 μm (Steglich et al. 2011). In the spectral region investigated in the present work, theory indicates several possible allowed transitions, $D_6(^2B_{2u}) \leftarrow D_0(^2B_{1g})$, $D_7(^2A_u) \leftarrow D_0(^2B_{1g})$, $D_8(^2B_{3u}) \leftarrow D_0(^2B_{1g})$, with oscillator strengths of $f \simeq 0.04$, 0.04 and 0.08, respectively. There is a weak feature from ~50 Å (also observed in 6 K neon matrix) to longer wavelengths than the strongest absorption that is also observed in 6 K neon matrix, which may thus arise due to vibronic coupling between electronic states.

The FWHM of the origin band at 8281 Å recorded with a laser bandwidth $\Delta\lambda \approx 0.2$ Å is around 3 Å. Given that the width due to the rotational profile of this large asymmetric top molecule is expected to be much smaller, see, e.g., Cossart-Magos & Leach (1990), the measured 3 Å FWHM is interpreted as arising from the lifetime of the excited electronic state(s), corresponding to a value of around a picosecond. While the matrix spectrum extends to wavelengths shorter than 7400 Å with numerous weak features, the gas-phase data were recorded only in the range 7690–8340 Å, encompassing the strongest bands.

Apart from a shift of around 30 Å the observed bands are nearly superimposable with those observed in the direct absorption measurement in the neon matrix at 6 K (Steglich et al. 2011). There are more resolved features in the gas-phase data, presumably as a result of broadening phenomena common to matrix isolation spectroscopy. Nevertheless, the similarities between these two spectra indicate that this is due to the ion with the HBC^+ structure. In a neon matrix isolation study carried out in our group using mass-selected $C_{42}H_{18}^{+}$ ions,[1] it was found that upon irradiation of the 5 K matrix with UV photons ($\lambda < 2700$ Å) this electronic system decreases in intensity and concurrently the known absorption systems of neutral HBC increase (Kokkin et al. 2008) at the same rate. This reversible inter-conversion indicates that the structure of $C_{42}H_{18}^{+}$ is closely related to that of HBC and thus the connectivity between the carbon atoms remains the same except for small changes in the C–C and C–H interatomic distances. The gas-phase data presented here from the ion trap measurements are not of the bare HBC^+ species itself because of the slight perturbation induced by the weakly bound helium atom; however, the shift is expected to be small. Laboratory data on the band at 8281 Å and the weak features near 8331 Å for $C_{42}H_{18}^{+}$–He_n ($n = 1, 2, 3$) are shown in Figure 2 and indicate that the helium causes a shift on the electronic transition of HBC^+ of around 0.4 Å. Considering the width of the absorption band profiles, for comparison with astronomical data, the spectrum of $C_{42}H_{18}^{+}$–He (Figure 1) can be considered to be that of the bare HBC^+ cation. In Table 1, the band maxima of the absorptions shown in Figure 1 are listed.

Steglich et al. (2011) predicted the gas-phase transition energies of HBC^+ based on their matrix data using a model (Gredel et al. 2011) to account for the polarizability of the different rare gases used. The present work enables a direct evaluation of this model and their results are also given in Table 1. The predicted values are found to be in accord with the gas phase; however, the large error bars (± 15 cm^{-1}) indicate that the extrapolation is not quite good enough for an unambiguous comparison with DIB data, especially if the latter are weak (EW $\simeq$ 10 mÅ). For this, gas-phase measurements as done here on $C_{42}H_{18}^{+}$ are required.

In the context of astronomical detectability it is important to determine the oscillator strength f of the individual transitions, in particular for the strongest band in the $C_{42}H_{18}^{+}$ spectrum. This is because the theoretically calculated values are not expected to be very accurate because of the nature of the method that had to be used (TD-DFT). Furthermore, these f values correspond to the the whole electronic absorption system(s). To obtain the oscillator strength for the origin band at 8281 Å, its Franck–Condon factor relative to all the other transitions has to be estimated, as carried out by Steglich et al. (2011). Thus, it is more reliable to measure absolute absorption cross sections directly in the ion trap, as previously demonstrated by measurements on the fullerene cations (Campbell et al. 2016a, 2017).

Absorption cross-section measurements were carried out at the wavelength of the band maxima of the two strongest absorptions in the $C_{42}H_{18}^{+}$–He spectrum. Plots showing typical exponential fits to the data are shown in Figure 3. The characteristic fluence, Φ_0, was found to be 0.8 and 0.9 mJ cm^{-2} at 8281 and 8248 Å, respectively. These values correspond to cross sections of $(3.0 \pm 1.2) \times 10^{-16}$ cm^2 and $(2.6 \pm 1.0) \times 10^{-16}$ cm^2. The latter are converted into oscillator strengths by numerically integrating over the absorption band profile, $f = \frac{m_e c^2}{\pi e^2} \int \sigma(\bar{\nu}) d\bar{\nu}$. This leads to f values of 2×10^{-3} and 3×10^{-3} for the features at 8281 and 8248 Å, in accord with the estimate given by Steglich et al. (2011). For comparison,

[1] Unpublished results from the Univ. Basel laboratory.

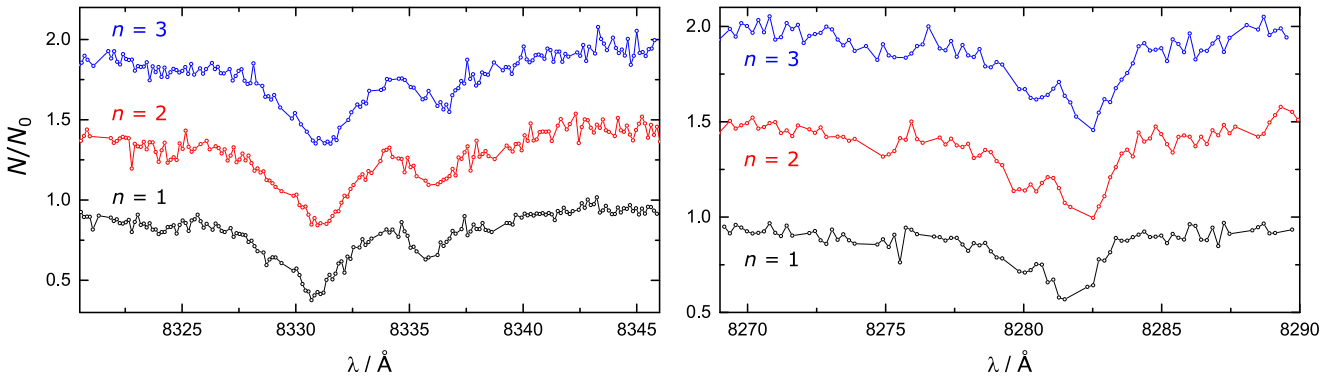

Figure 2. Electronic spectra of $C_{42}H_{18}^{+}$–He_n (n = 1–3) below 10 K. Data are shown for two of the bands presented in Figure 1. The similarities between the n = 1–3 spectra indicate that the shift on the electronic transition of $C_{42}H_{18}^{+}$ due to the presence of the helium is small. Therefore, the spectrum of $C_{42}H_{18}^{+}$–He may be regarded as that of $C_{42}H_{18}^{+}$ for comparison with DIB data. A linear offset has been applied to the vertical axis of the n = 2–3 data shown.

Table 1
Absorption Maxima of the Bands Shown in Figure 1 and Compared with the $C_{42}H_{18}^{+}$ Gas-phase Prediction Reported by Steglich et al. (2011)

Steglich et al. (2011)	This Work[a]	
$\bar{\nu}$/cm^{-1}	$\bar{\nu}$/cm^{-1}	Å
⋯	12000	8331
12084 ± 14	12072	8281
⋯	12082	8274
⋯	12103	8260
12137 ± 13	12121	8248
⋯	12238	8169
⋯	12284	8138
12364 ± 16	12384	8073
⋯	12395	8066
⋯	12436	8039
⋯	12499	7998
12584 ± 16	12558	7961
12597 ± 16	12573	7951
12618 ± 16	12606	7931
⋯	12653	7901
12843 ± 16	12829	7793
12934 ± 17	12937	7728
	±1 cm^{-1}	±1 Å

Note.
[a] Weak absorptions with intensities lower than 20% of the band at 12072 cm^{-1} are not listed.

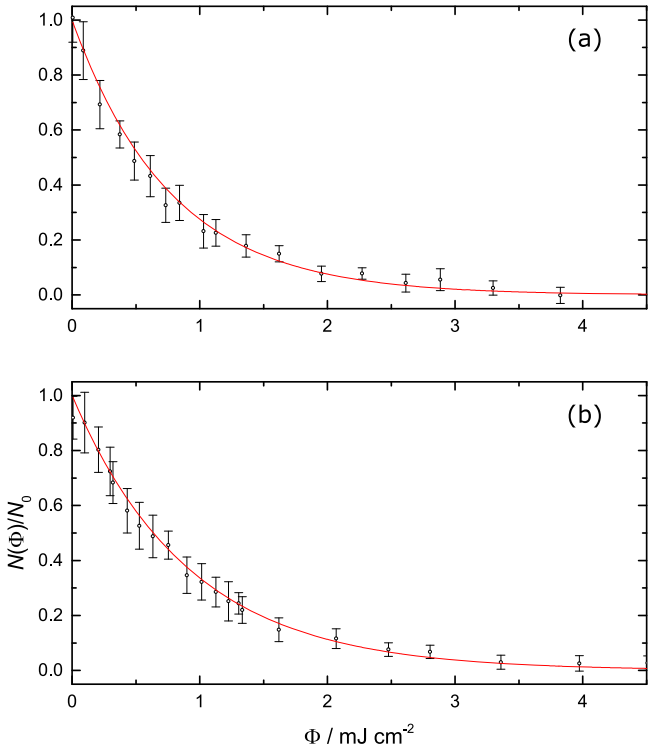

Figure 3. Photofragmentation of $C_{42}H_{18}^{+}$–He as a function of laser fluence at (a) λ = 8281 Å and (b) λ = 8248 Å. Experimental data (circles) were fit with exponential functions (lines), providing information on the photofragmentation cross section. The data were corrected for the same number of background ions appearing at m/z = 526 u/e.

the latter study reports 6.5 × 10^{-3} and 3.2 × 10^{-3} with errors $^{+20\%}_{-60\%}$, respectively.

4. Astrophysical Implications

In the available DIB compilation covering this wavelength range, by Galazutdinov et al. (2000), there is no absorption at the wavelength of the origin band of HBC^{+} or at the strong band at 8248 Å. The upper limit to the column density can be calculated using the f(0–0) = 2 × 10^{-3} value determined experimentally and the detection limits of the DIB catalog. Galazutdinov et al. (2000) do not explicitly state their detection limits. The survey by Hobbs et al. (2008) indicates that an equivalent width (EW) of about 7 mÅ would be detected near this region for a band with a FWHM of 3 Å; however, their survey does not extend to wavelengths longer than 8000 Å. In the following discussion we assume that a DIB EW of 10 mÅ would have been detected.

The column density can be evaluated using

$$N(C_{42}H_{18}^{+}) = 10^{8}\frac{m_e c^2}{\pi e^2}\frac{\mathrm{EW}_\lambda}{\lambda^2 f}. \quad (1)$$

With values of λ_c = 8281 Å, EW_λ = 1 × 10^{-2} Å, and f = 2 × 10^{-3} an upper limit to the abundance of HBC^{+} is calculated to be 8 × 10^{12} cm^{-2}. By contrast, recently it was shown that the column density of the C_{60}^{+} in diffuse clouds is 2 × 10^{13} cm^{-2} (Campbell et al. 2016a).

Measurements of the fragmentation of PAH^{+} species have led to the conclusion that those comprising less than about

40–50 carbon atoms are likely to lose their hydrogen atoms, an example being the coronene cation, $C_{24}H_{12}^{+}$ (Ekern et al. 1998). In the case of HBC^{+} experiments by Zhen et al. (2015), it was shown that at energies limited to 13.6 eV, photoionization dominates over fragmentation.

5. Conclusions

Gas-phase measurement of the near-infrared electronic spectrum of the hexabenzocorone cation, $C_{42}H_{18}^{+}$, below 10 K is reported. To date, this represents the spectrum of the largest PAH cation to be observed at sufficient quality, in the gas phase, to enable a direct comparison with astronomical data. Absorption cross-section measurements allow upper limits on the column density of HBC^{+} in diffuse clouds to be placed (10^{12} cm^{-2}) without the need to rely on theoretical oscillator strengths. These findings quantify the results reported in the matrix isolation study by Steglich et al. (2011), who stressed that there is no evidence to suggest that any of the neutral or ionized PAHs studied so far are responsible for any of the strong DIBs. This conclusion remains valid following gas-phase measurement of HBC^{+}, a PAH cation containing 60 atoms that is predicted to be stable in the diffuse medium. If PAH^{+} are present in these environments with column densities of 10^{12}–10^{13} cm^{-2}, then in order to be detectable as DIBs a much larger electronic oscillator strength for the strongest absorptions is required.

References

Campbell, E. K., Holz, M., Gerlich, D., & Maier, J. P. 2015, Natur, 523, 322
Campbell, E. K., Holz, M., Maier, J. P., et al. 2016a, ApJ, 822, 17
Campbell, E. K., Holz, M., & Maier, J. P. 2016b, ApJL, 826, L4
Campbell, E. K., Holz, M., & Maier, J. P. 2017, ApJ, 835, 221
Cossart-Magos, C., & Leach, S. 1990, A&A, 233, 559
Ekern, S. P., Marshall, A. G., Szczepanski, J., & Vala, M. 1998, JPCA, 102, 3498
Galazutdinov, G. A., Musaev, F. A., Krewlowski, J., & Walker, G. A. H. 2000, PASP, 112, 648
Gredel, R., Carpentier, Y., Rouillé, G., et al. 2011, A&A, 530, A26
Hardy, F.-X., Rice, C. A., & Maier, J. P. 2017, ApJ, 836, 37
Hobbs, L. M., York, D. G., Snow, T. P., et al. 2008, ApJ, 680, 1256
Kokkin, D. L., Troy, T. P., Nakajima, M., et al. 2008, ApJL, 681, L49
Le Page, V., Snow, T. P., & Bierbaum, V. M. 2003, ApJ, 584, 316
Steglich, M., Bouwman, J., Huisken, F., & Henning, Th. 2011, ApJ, 742, 1
Tielens, A. G. G. M. 2008, ARA&A, 46, 289
Walker, G. A. H., Campbell, E. K., Maier, J. P., & Bohlender, D. 2017, ApJ, 843, 56
Zhen, J., Castellanos, P., Paardekooper, D. M., et al. 2015, ApJL, 804, L7
Zhen, J., Mulas, G., Bonnamy, A., & Joblin, C. 2016, MolAs, 2, 12